

# A COMPACT, LOW-FIELD, BROADBAND MATCHING SECTION FOR EXTERNALLY-POWERED X-BAND DIELECTRIC-LOADED ACCELERATING STRUCTURES

Y. Wei<sup>1,†</sup>, A. Grudiev, N. Catalan-Lasheras, R. Wegner, S. Gonzalez Anton, CERN, Geneva, Switzerland

C. Jing, B. Freemire, Euclid TechLabs LLC, Solon, USA

H. Bursali, Sapienza University of Rome, Rome, Italy

J. Sauza-Bedolla, Lancaster University, Lancaster, UK

C. P. Welsch, Cockcroft Institute and University of Liverpool, Liverpool, UK

<sup>1</sup>also at Cockcroft Institute and University of Liverpool, Liverpool, UK

## Abstract

It has been technically challenging to efficiently couple external radiofrequency (RF) power to cylindrical dielectric-loaded accelerating (DLA) structures. This is especially true when the DLA structure has a high dielectric constant. This paper presents a novel design of a matching section for coupling the RF power to an X-band DLA structure with a dielectric constant  $\epsilon_r = 16.66$  and a loss tangent  $\tan \delta = 3.43 \times 10^{-5}$ . It consists of a very compact dielectric disk with a width of 2.035 mm and a tilt angle of  $60^\circ$ , resulting in a broadband coupling at a low RF field which has the potential to survive in the high-power environment. To prevent a sharp dielectric corner break, a  $45^\circ$  chamfer is added. Moreover, a microscale vacuum gap, caused by metallic clamping between the thin coating and the outer thick copper jacket, is studied in detail. Based on simulation studies, a prototype of the DLA structure with the matching sections was fabricated. Results from preliminary bench measurements and their comparison with design values will also be discussed.

## INTRODUCTION

Dielectric-loaded accelerating (DLA) structures, utilizing dielectrics to slow down the phase velocity of travelling waves in the vacuum channel, have been studied both theoretically [1, 2] and experimentally [3, 4] as a potential alternative to conventional RF structures. A DLA structure comprises a simple geometry where a uniform and linear dielectric tube is surrounded by a conducting cylinder. The simplicity of DLA structures offers great advantages for fabrication of high frequency accelerating structures, as compared with conventional RF structures which demand extremely tight fabrication tolerances. This is of great importance in the case of linear colliders, where tens of thousands of accelerating structures have to be built. However, there are still some potential challenges for DLA structures, such as breakdown [5] and multipacting [5-7]. In addition to these challenges, a practical issue to be addressed is the efficient coupling of the RF power into a DLA structure with an outer diameter much smaller than the waveguide. We present in this paper a novel design of a matching section for efficiently coupling the RF power from a circular

waveguide to an X-band DLA structure. There are 3 modules in the scheme: TE<sub>10</sub>-TM<sub>01</sub> mode converters with choke geometry, matching sections, and the DLA structure, as shown in Fig. 1. The mode converter has been studied in detail [8, 9], so we concentrate our efforts on the design of the matching section and DLA structure with the aim to achieve the broadband coupling with the maximum fields located at the DLA structure. Based on simulation studies, the prototypes of a DLA structure with the matching sections and the mode converters are obtained after fabrication. The RF bench measurements are carried out for the assembly of the whole structure.

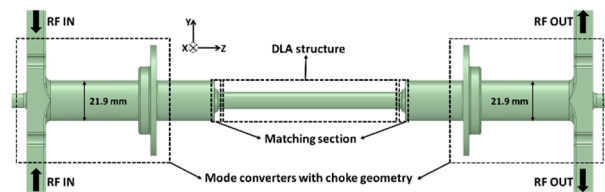


Figure 1: Conceptual illustration of an externally-powered DLA structure with matching sections.

## DESIGN OF AN X-BAND DLA STRUCTURE

In this section, the RF properties of an X-band DLA structure (see Fig. 2) are studied in detail.

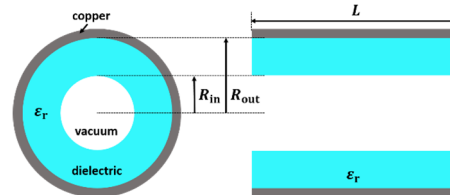


Figure 2: Front view and longitudinal cross section of a cylindrical DLA structure.

MgTiO<sub>3</sub> ceramic, with good thermal conductivity and ultralow power loss, which has been studied in [10], is chosen as the dielectric material for our DLA structure. An accurate measurement of the dielectric properties has to be performed before using such a ceramic for our RF design. As shown in Fig. 3, a TE<sub>018</sub> silver-plated resonator, which is designed for testing ceramics at an X-band frequency, is used to measure the dielectric constant  $\epsilon_r$  and loss tangent

<sup>†</sup> yelong.wei@cern.ch

Content from this work may be used under the terms of the CC BY 3.0 licence (© 2021). Any distribution of this work must maintain attribution to the author(s), title of the work, publisher, and DOI

$\tan\delta$  of sample coupons. Four coupons made from the same dielectric rods as for the fabrication are measured. A dielectric constant  $\epsilon_r = 16.66$  and a loss tangent  $\tan\delta = 3.43 \times 10^{-5}$  (having error bars 0.6% of the nominal value) are obtained for the RF design of the DLA structure and matching sections which follows.

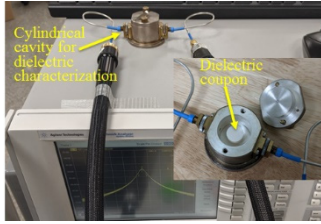


Figure 3: Measurement setup of the dielectric properties.

The DLA structure could be potentially used for the CLIC main linac. The inner radius is chosen to be  $R_{in} = 3.0$  mm from consideration of the CLIC beam dynamics requirement [11, 12]. The outer radius is then calculated to be  $R_{out} = 4.6388$  mm for an operating frequency of  $f_0 = 11.994$  GHz. The group velocity obtained is  $v_g = 0.066c$ , where  $c$  is speed of light. A quality factor of  $Q_0 = 2829$  and a shunt impedance of  $R_{shunt} = 26.5$  M $\Omega$ /m are also derived for such a DLA structure. The length of the DLA structure is chosen as  $L = 100$  mm for the following simulations and mechanical assembly.

## DESIGN OF A MATCHING SECTION

In this section, a dielectric matching section to efficiently couple the RF power from a circular waveguide into the DLA structure will be presented and analyzed in detail.

### A Chamfered Dielectric Matching Section

After optimization, a compact, low-field, broadband matching section with a tilt angle of  $\theta = 60^\circ$  is obtained. In realistic fabrication, a sharp dielectric corner easily breaks. In order to prevent such a break, a  $45^\circ$  chamfer with a length of 0.254 mm is added to this corner, as shown in Fig. 4.

Figure 4 (left) shows the calculated electric field distribution for the chamfered dielectric matching section at an input power of 1 W. Figure 4 (right) indicates that the electric fields near that area are much lower than those of the DLA structure. In this case, this dielectric matching section has the potential to withstand high-power test.

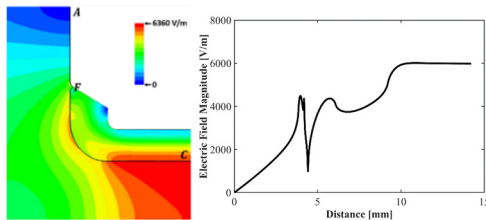


Figure 4: (left) Electric field distribution for chamfered dielectric matching section. (right) Electric field magnitude along Line AFC, where the distance of point A is taken as 0 mm.

Figure 5 shows the calculated  $S_{11} = -54$  dB and  $S_{21} = -0.03$  dB for the chamfered dielectric matching section. It has a coupling coefficient of 99.3% and  $S_{21}$  also has a broad 3 dB bandwidth of more than 1 GHz.

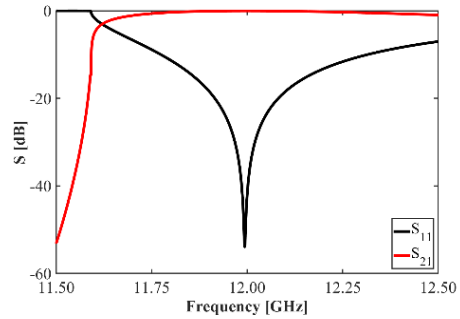


Figure 5: Simulated  $S_{11}$  and  $S_{21}$  as a function of frequency for the chamfered dielectric matching section.

### A Vacuum Microgap

A thin metallic layer of  $d_1 = 0.0508$  mm is coated onto the surface of the whole dielectric tube which is then inserted into the outer two-halves copper jacket. However, there is a vacuum microgap  $d_2$  caused by metallic clamping between the thin coating and the copper jacket, as shown in Fig. 6. It is therefore necessary to study the dependence of the S-parameters on this microgap  $d_2$ .

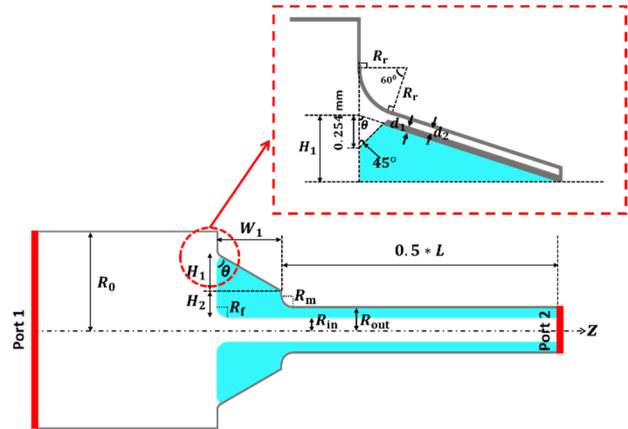


Figure 6: Geometry of a chamfered dielectric matching section with a vacuum microgap, and a DLA structure.

Figure 7 shows how varying  $d_2$  influences  $S_{11}$  and  $S_{21}$ . With a larger  $d_2$ ,  $S_{11}$  increases while  $S_{21}$  decreases, resulting in worse matching. For a vacuum microgap of 0.3 mm, the peak fields are found to be higher than those of the DLA structure, which may cause arcing in the high-power test. The dielectric matching section is therefore allowed to have a maximum vacuum microgap of 0.2 mm, in which RF fields are still lower than those of DLA structure,  $S_{11}$  is better than -30 dB, and the coupling coefficient is 93%.

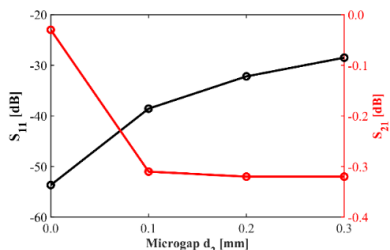


Figure 7: Simulated  $S_{11}$  and  $S_{21}$  as a function of vacuum microgap  $d_2$ .

### Tolerance Studies

The optimum geometry (see Fig. 6) for the matching section and the DLA structure is listed in Table 1. The tolerances are studied: By adjusting a certain parameter from  $x$  to  $x \pm dx$ ,  $S_{11}$  is calculated and compared with the setting requirement of -20 dB. It can be seen from Table 1 that  $S_{11}$  is very sensitive to  $W_1$ ,  $R_{out}$ , and  $R_{in}$  and less sensitive to  $\epsilon_r$ ,  $H_2$ ,  $\theta$ ,  $R_f$ , and  $R_m$ . The dielectric fabrication accuracy should be better than  $\pm 0.02$  mm in order to realize a  $S_{11} \leq -20$  dB, which is acceptable for efficient coupling.

Table 1: Geometric Tolerance Studies

$f_0 = 11.994$ GHz	$S_{11} \leq -20$ dB
$\epsilon_r = 16.66$	[-0.24, +0.27]
$W_1 = 2.035$ [mm]	[-0.022, +0.022]
$H_2 = 2.74$ [mm]	[-0.051, +0.054]
$\theta = 60^\circ$	[-7.3°, +7.0°]
$R_f = 2.0$ [mm]	[-0.140, +0.120]
$R_m = 0.5$ [mm]	[-0.245, +0.151]
$R_{out} = 4.6388$ [mm]	[-0.020, +0.025]
$R_{in} = 3.0$ [mm]	[-0.024, +0.020]

### Full-assembly Structure

The mode converters with choke geometry, the matching sections and the DLA structure are connected together as a full-assembly structure in simulation, as shown in Fig. 8. The electric field distribution is simulated for the whole structure when the RF power transmits from Port 1' to Port 2'.

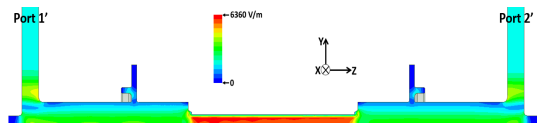


Figure 8: Simulated electric field distribution for the full-assembly structure.

### PRELIMINARY LOW-POWER TESTING

After fabrication, the prototypes of the DLA structure with the matching sections and mode converters are obtained. As shown in Fig. 9 (left), the fabricated dielectric structure has a thin silver coating on its surface which is clamped by two-halves copper jacket. It is then assembled with the fabricated mode converters, as shown in Fig. 9 (right).

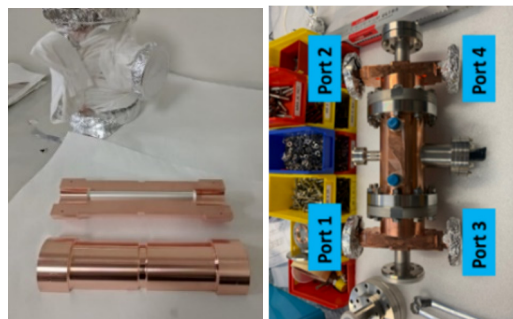


Figure 9: The prototype of (left) the DLA structure and (right) the mechanical assembly of the whole structure.

The full-assembly structure is then connected with a 4-port network analyser for low-power testing. As shown in Fig. 10, the measured  $S'_{11} = -11.35$  dB and  $S'_{21} = -6.34$  dB while the simulated  $S'_{11} \leq -40$  dB and  $S'_{21} = -0.67$  dB at the designed frequency of 11.994 GHz. It is obvious that there is a significant discrepancy between measurements and simulations. This discrepancy may be caused by fabrication errors for the DLA structure with the matching sections. Investigations into possible reasons for the discrepancy are ongoing.

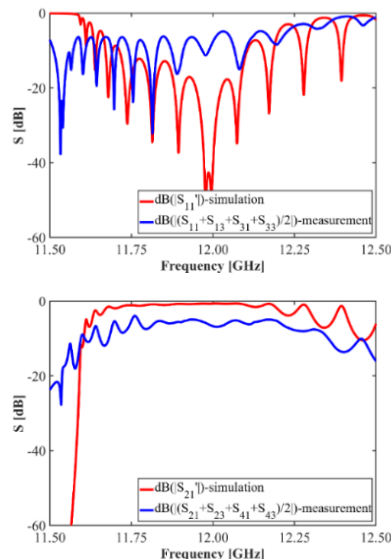


Figure 10: Comparison between measured and simulated S-parameters.

### CONCLUSION

A compact, low-field, broadband matching section has been proposed and studied to efficiently couple the RF power from a circular waveguide to an X-band DLA structure in detail. A prototype of the DLA structure with the matching sections was subsequently built and mechanically assembled with the mode converters. Preliminary RF bench measurements have been carried out for the whole structure. A significant discrepancy, probably due to fabrication errors, was found between measured and simulated S-parameters. Further investigations are being performed to understand the origin of these differences.

## REFERENCES

- [1] R. B. R. S. Harvie, "A proposed new form of dielectric-loaded wave-guide for linear electron accelerators", *Nature*, vol. 162, p. 890, Dec. 1948. doi:10.1038/162890a0
- [2] S. Y. Park and J. L. Hirshfield, "Theory of wakefields in a dielectric-lined waveguide", *Phys. Rev. E.*, vol. 62, pp. 1266-1283, July 2000. doi:10.1103/PhysRevE.62.1266
- [3] G. B. Walker and E. L. Lewis, "Vacuum Breakdown in Dielectric-loaded Wave-guides", *Nature*, vol. 181, pp. 38-39, Jan. 1958. doi:10.1038/181038b0
- [4] W. Gai *et al.*, "Experimental demonstration of wake-field effects in dielectric structures", *Phys. Rev. Lett.*, vol. 61, no. 24, pp. 2756-2758, Dec. 1988. doi:10.1103/PhysRevLett.61.2756
- [5] C. Jing *et al.*, "High-power RF tests on X-band dielectric-loaded accelerating structures", *IEEE T. Plasma Sci.*, vol. 33, no. 4, pp. 1155-1160, Aug. 2005. doi:10.1109/TPS.2005.851957
- [6] J. G. Power *et al.*, "Observation of multipactor in an alumina-based dielectric-loaded accelerating structure", *Phys. Rev. Lett.*, vol. 92, no. 16, p. 164801, Apr. 2004. doi:10.1103/PhysRevLett.92.164801
- [7] C. Jing, S. H. Gold, R. Fischer, and W. Gai, "Complete multipactor suppression in an X-band dielectric-loaded accelerating structure", *Appl. Phys. Lett.*, vol. 108, no. 19, p. 193501, May 2016. doi:10.1063/1.4949334
- [8] I. Syrathev, "Mode launcher as an alternative approach to the cavity-based RF coupler of periodic structures", CERN, Geneva, Switzerland, Rep. CERN-OPEN-2002-005, Jan. 2002.
- [9] Y. Wei *et al.*, "A compact, low field, broadband matching section for externally-powered X-band dielectric-loaded accelerating structures", 2020. arxiv:2008.09203
- [10] A. Kanareykin, "New advanced dielectric materials for accelerator applications", *AIP Conf. Proc.*, vol. 1299, pp. 286-291, Nov. 2010. doi:10.1063/1.3520329
- [11] A. Grudiev and W. Wuensch, "Design of the CLIC main linac accelerating structure for CLIC Conceptual Design Report", in *Proc. 25th Linear Accelerator Conf. (LINAC'10)*, Tsukuba, Japan, Sep. 2010, paper MOP068, pp. 211-213.
- [12] H. Zha and A. Grudiev, "Design and optimization of Compact Linear Collider main linac accelerating structure", *Phys. Rev. Accel. Beams*, vol. 19, p. 111003, Nov. 2016. doi:10.1103/PhysRevAccelBeams.19.111003